

Magnetic, transport and magnetotransport properties of $\text{Mn}_{3+x}\text{Sn}_{1-x}\text{C}$ and $\text{Mn}_3\text{Zn}_y\text{Sn}_{1-y}\text{C}$ compounds

Y. B. Li, W. F. Li, W. J. Feng, Y. Q. Zhang, and Z. D. Zhang

Shenyang National Laboratory for Materials Science, Institute of Metal Research, and International Centre for Materials Physics, Chinese Academy of Sciences, 72 Wenhua Road, Shenyang 110016, People's Republic of China

(Received 26 April 2004; published 1 July 2005)

The magnetic, transport, and magnetotransport properties of $\text{Mn}_{3+x}\text{Sn}_{1-x}\text{C}$ ($0 \leq x \leq 0.4$) and $\text{Mn}_3\text{Zn}_y\text{Sn}_{1-y}\text{C}$ ($0 \leq y \leq 0.9$) compounds are investigated systematically. For $\text{Mn}_{3+x}\text{Sn}_{1-x}\text{C}$, a sharp rise in temperature dependence of resistivity is observed for $x \leq 0.1$, accompanied by a magnetic phase transition from a paramagnetic state to a complicated spin arrangement composed of antiferromagnetic and ferromagnetic sublattices. A different behavior appears in the resistivity of $\text{Mn}_{3.2}\text{Sn}_{0.8}\text{C}$, which decreases monotonically with decreasing temperature. A partial Zn substitution for Sn in Mn_3SnC leads to dramatic changes of magnetic and transport properties. As the temperature decreases, a magnetic transition from the ferromagnetic (or ferrimagnetic) to antiferromagnetic state occurs at about 170 and 142 K for $\text{Mn}_3\text{Zn}_{0.4}\text{Sn}_{0.6}\text{C}$ and $\text{Mn}_3\text{Zn}_{0.5}\text{Sn}_{0.5}\text{C}$ compounds, respectively, which strongly affects their transport properties. A significant magnetoresistance as large as 34% is observed for $\text{Mn}_3\text{Zn}_{0.5}\text{Sn}_{0.5}\text{C}$ at 95 K, in accordance with a field-induced metamagnetic transition. The origin of the magnetoresistance effect is discussed in terms of the reconstruction of the Fermi surface.

DOI: [10.1103/PhysRevB.72.024411](https://doi.org/10.1103/PhysRevB.72.024411)

PACS number(s): 75.47.De, 75.47.Np, 75.50.Ee, 75.50.Gg

I. INTRODUCTION

Since the discovery of the giant magnetoresistance (GMR) in antiferromagnetic coupled Fe/Cr multilayers,¹ the GMR effect has attracted much interest, which has been subsequently observed in many multilayer systems,²⁻⁴ and granular films.^{5,6} The large magnetoresistance has been found also in intermetallic compounds NdCu_2 , FeRh , UNiGa , and UPdIn , etc.⁷ After recent observation of magnetoresistance (MR) phenomenon in Mn_3GaC (Refs. 8 and 9) and superconductivity in MgCNi_3 ,¹⁰ compounds with the antiperovskite structure have attracted great attention. A family of ternary manganese compounds with a formula of Mn_3MC (M=Al, Ga, Zn, In, and Sn) have the cubic crystal structure of a perovskite-type:¹¹⁻¹⁴ The Mn atoms are located on the face centered positions, the M atoms on the cubic corners, and the C atom at the body centered position. In spite of the simple crystal structure, these compounds show a wide variety of magnetic moments, structures, and transitions. In particular, we realize that the antiperovskite manganese compounds that exhibit intriguing magnetic structures¹¹⁻¹⁴ might show abnormal transport and magnetotransport properties. The aim of this work is to explore these properties of $\text{Mn}_{3+x}\text{Sn}_{1-x}\text{C}$ ($0 \leq x \leq 0.4$) and $\text{Mn}_3\text{Zn}_y\text{Sn}_{1-y}\text{C}$ ($0 \leq y \leq 0.9$) compounds.

In the case of Mn_3SnC , a complicated spin arrangement,¹² i.e., a noncollinear ferrimagnetic (FI) state, consisting of antiferromagnetic (AFM) and ferromagnetic (FM) sublattices, exists up to its Curie temperature T_C , 265 K.^{13,15-18} With increasing temperature, the transition to the paramagnetic (PM) state is accompanied by a discontinuous disappearance of magnetization and an abrupt contraction on lattice parameter without a change of the type of the crystal structure.^{13,14} The results of neutron diffraction showed that the magnetic moments of Mn atoms are much smaller than $4 \mu_B$ observed in other ordered manganese alloys, indicating a strong itin-

erant character of d electrons of the Mn atoms in Mn_3MC .¹⁸

In this paper, the magnetic, transport, and magnetotransport properties of $\text{Mn}_{3+x}\text{Sn}_{1-x}\text{C}$ ($0 \leq x \leq 0.4$) and $\text{Mn}_3\text{Zn}_y\text{Sn}_{1-y}\text{C}$ ($0 \leq y \leq 0.9$) compounds will be investigated systematically. Section II gives the experimental details. The results and discussion for $\text{Mn}_{3+x}\text{Sn}_{1-x}\text{C}$ and $\text{Mn}_3\text{Zn}_y\text{Sn}_{1-y}\text{C}$ compounds are represented in Secs. III A and III B, respectively. In Sec. III A, the temperature dependence of electrical resistance in $\text{Mn}_{3+x}\text{Sn}_{1-x}\text{C}$ compounds will be investigated, to clarify the origin of the change in the resistivity associated with the magnetic phase transition. In addition, in order to obtain a single and stable AFM phase at low temperatures and correspondingly to occur a magnetic phase transition from FM (or FI) to the AFM state, which are important for the appearance of a large MR effect, we shall study the effect of Zn substitution for Sn on magnetic, transport, and magnetotransport properties in Sec. III B. We shall demonstrate the magnetic phase transition and the MR effect in $\text{Mn}_3\text{Zn}_y\text{Sn}_{1-y}\text{C}$ compounds, and discuss the origin of these behaviors. The temperature dependence of the resistivities at zero field and at a magnetic field of 5 and 12 T, and the MR ratio of $\text{Mn}_3\text{Zn}_{0.5}\text{Sn}_{0.5}\text{C}$ and $\text{Mn}_3\text{Zn}_{0.4}\text{Sn}_{0.6}\text{C}$ compounds as well as the field dependence of the magnetoresistance and the magnetization of the $\text{Mn}_3\text{Zn}_{0.5}\text{Sn}_{0.5}\text{C}$ compound at different temperatures are represented.

II. EXPERIMENTAL DETAILS

Polycrystalline samples of $\text{Mn}_{3+x}\text{Sn}_{1-x}\text{C}$ ($0 \leq x \leq 0.4$) and $\text{Mn}_3\text{Zn}_y\text{Sn}_{1-y}\text{C}$ ($0 \leq y \leq 0.9$) were prepared from Mn, Sn, Zn with purity of 99.9% and spectroscopic grade carbon powders. The starting materials were mixed in the desired proportion and pressed into pellets. The pellets were placed into Al_2O_3 crucibles that were sealed in an evacuated silica tube. The samples were heated at 800 °C for seven days. After

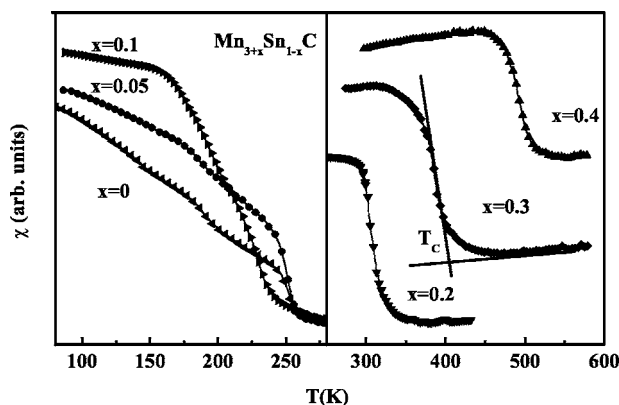


FIG. 1. Temperature dependence of the susceptibility of $\text{Mn}_{3+x}\text{Sn}_{1-x}\text{C}$ compounds.

cooling, they were pulverized, mixed, pressed into pellets, and heated again under the same conditions, because one procedure did not homogenize the samples perfectly. X-ray diffraction (XRD) studies were carried out at room temperature with $\text{Cu } K_\alpha$ radiation in a $D/\text{max-}\gamma\text{A}$ diffractometer with a graphite crystal monochromator, which certified that all the samples displayed peaks characteristic for the cubic perovskite-type structure. X-ray diffraction studies at low temperatures were carried out by PW1700 x-ray diffractometer. The temperature dependence of the ac initial susceptibility was applied to determine the Curie temperature and the temperatures of the magnetic phase transitions. The sintered polycrystalline samples were cut into a bar shape ($1 \text{ mm} \times 1 \text{ mm} \times 8 \text{ mm}$) for measurements of transport properties. A physical property measurement system (PPMS) was employed to collect the magnetization data. Magnetotransport measurements were accomplished using a standard four-probe method with a dc current perpendicular to magnetic fields.

III. RESULTS AND DISCUSSION

A. $\text{Mn}_{3+x}\text{Sn}_{1-x}\text{C}$ ($0 \leq x \leq 0.4$)

The temperature dependence of the ac initial susceptibility of $\text{Mn}_{3+x}\text{Sn}_{1-x}\text{C}$ compounds is shown in Fig. 1, while the Mn—Mn distance and Curie temperature T_C of all compounds are shown in Fig. 2. The Curie temperature T_C is determined to be the crossing point of two tangent lines of the susceptibility curve (see Fig. 1). Mn—Mn distance is calculated by $\sqrt{2}/2$ times the lattice parameter. Butters and Myers suggested that for the compounds with the composition of $\text{Mn}_{3+x}\text{Sn}_{1-x}\text{C}$, the excess x manganese atoms occupy the position of the cube corners of the perovskite unit cell.¹⁹ As seen in Fig. 2, the Mn—Mn distance (as well as the lattice parameter) decreases with increasing Mn concentration, while the Curie temperature of the FI compounds increases with the decrease of the lattice parameter. This means that the coupling of magnetic moments increases with the decrease of the Mn—Mn distance.¹⁹

Figure 3 represents the temperature dependence of the resistivity for $\text{Mn}_{3+x}\text{Sn}_{1-x}\text{C}$ ($x=0, 0.05, 0.1, \text{ and } 0.2$) compounds. The overall behaviors of the resistivities for the

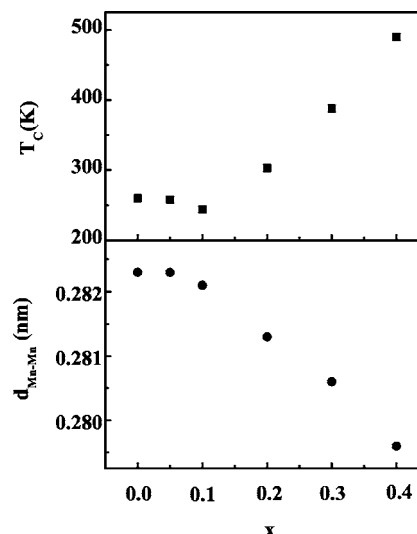


FIG. 2. Composition dependence of Mn—Mn distance and Curie temperature of $\text{Mn}_{3+x}\text{Sn}_{1-x}\text{C}$ compounds.

Mn_3SnC and $\text{Mn}_{3.05}\text{Sn}_{0.95}\text{C}$ compounds are alike, in which the resistivities first decrease with decreasing the temperature, then rise abruptly at a certain temperature (260 K for Mn_3SnC and 258 K for $\text{Mn}_{3.05}\text{Sn}_{0.95}\text{C}$) to reach a maximum, and finally decrease with a further decrease in temperature. A broader maximum is observed in the temperature dependence of resistivity for the $\text{Mn}_{3.05}\text{Sn}_{0.95}\text{C}$ compound. For the $\text{Mn}_{3.1}\text{Sn}_{0.9}\text{C}$ compound, the variation of resistivity shows a semiconductorlike transport property. In all three compounds above, there exists an anomalous increase in resistivity at a certain temperature that is in good agreement with their Curie temperature T_C (i.e., the transition temperature $T_{\text{PM-FI}}$). Namely, these abnormal behaviors originate from a transition from the PM state to the FI state. At the same time, abrupt changes can be observed in the temperature dependence of the lattice parameter at about 260 and 250 K for Mn_3SnC and $\text{Mn}_{3.1}\text{Sn}_{0.9}\text{C}$, respectively, just corresponding to their Curie temperature T_C (see Fig. 4). As we know, the abrupt change of the crystal structure and the lattice parameter may result from the shift of the Fermi energy surface from one Brillouin zone (BZ) to another one. As reported early,¹⁸ the density of state (DOS) of Mn_3SnC showed that the Fermi level lies just above a sharp peak of the DOS. This implies that a small shift of the Fermi energy surface can result in an abrupt decrease of the DOS near the Fermi level, which could lead to a pronounced decrease of the effective number of conduction electrons. Correspondingly, the resistivity could be enhanced significantly at the transition temperature for Mn_3SnC , $\text{Mn}_{3.05}\text{Sn}_{0.95}\text{C}$, and $\text{Mn}_{3.1}\text{Sn}_{0.9}\text{C}$. For Mn_3SnC and $\text{Mn}_{3.05}\text{Sn}_{0.95}\text{C}$, the total transport behavior is metallic, namely, the resistivity decreases with decreasing temperature after the abrupt increment at the transition temperature. For $\text{Mn}_{3.1}\text{Sn}_{0.9}\text{C}$, however, semicon-

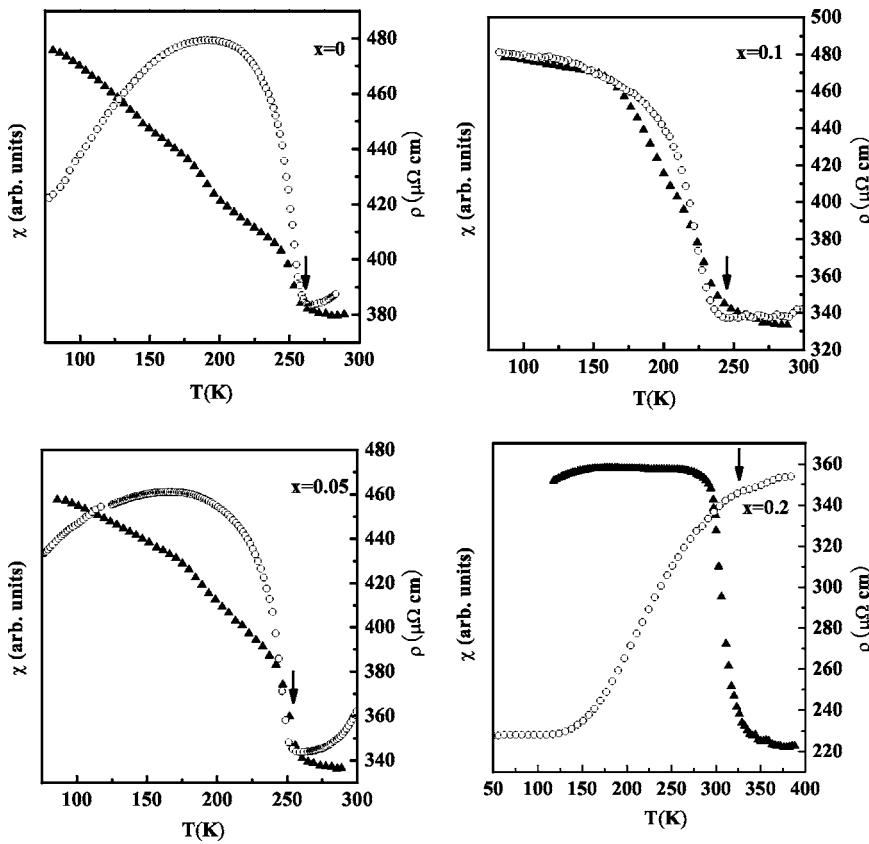


FIG. 3. Temperature dependence of the resistivity (circles) and the susceptibility (triangles) of $Mn_{3+x}Sn_{1-x}C$ compounds ($x = 0, 0.05, 0.1,$ and 0.2). The arrows indicate the Curie temperature T_C .

ductorlike transport behavior may result from the change of its energy band structure, possibly the formation of the energy gap, which needs to be confirmed further by the first principle calculation.

However, a totally different behavior in temperature dependence of resistivity is observed for the $Mn_{3.2}Sn_{0.8}C$ compound, which decreases monotonically with decreasing temperature. Above the Curie temperature T_C , the slope ($d\rho/dT$) is small. With decreasing the temperature, there is an obvious increase of the slope below the transition temperature. Such difference in the transport behavior with the change of the Mn content can be interpreted as follows: With a further

increase of Mn concentration (for $x > 0.1$), the electron density in the system increases further. As a result, the Fermi radius increases and the Fermi surface enters the next BZ directly. Thus, in the case of $Mn_{3.2}Sn_{0.8}C$, there is no abrupt change of the DOS on the Fermi energy level as well as of the resistivity. The variation in the resistivity for the $Mn_{3.2}Sn_{0.8}C$ compound can be explained by the magnetic scattering mechanism. It is a fundamental fact in condensed matter physics that in metals containing magnetic moments, besides the lattice contribution to the electrical resistivity (ρ), which decreases with decreasing the temperature, a constant spin-disorder contribution exists in the PM state. In FM (or FI) state, the orientation of the magnetic moments becomes ordered and the transport electrons suffer smaller scattering probability than that in the PM state. As a consequence, the mean free path of electrons becomes longer and the resistance decreases rapidly.

From the particular observations above, we can conclude that Mn in these compounds is primarily responsible for their quite unusual transport properties. Then, it is interesting to study the magnetotransport properties of these compounds. The field-dependent resistivity of the Mn_3SnC and $Mn_{3.1}Sn_{0.9}C$ compounds is shown in Fig. 5 for fields up to 5 T. Obviously, the magnetic fields do not significantly change the overall resistivity behavior. In both cases, the MR does not exceed values of about 4% at the critical temperatures. The positive magnetoresistance and the very small changes of resistivity in a reasonably large field exclude the magnetic scattering processes as the principle interaction mechanism in these two compounds.

From the results above, one can see that near the Curie temperature, no field-induced metamagnetic phase transition

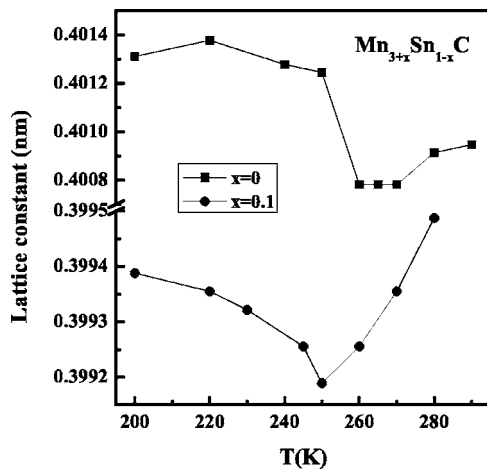


FIG. 4. Temperature dependence of the lattice parameter of Mn_3SnC and $Mn_{3.1}Sn_{0.9}C$.

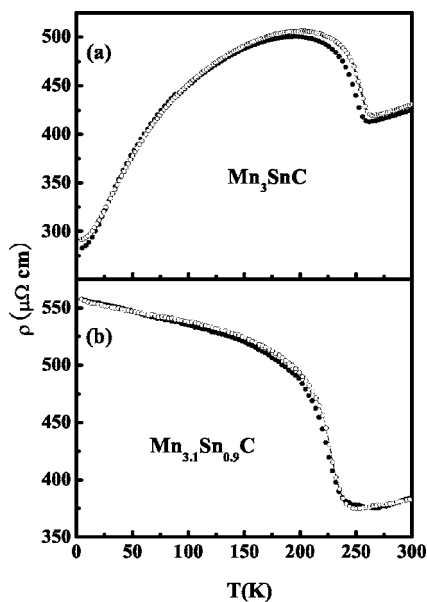


FIG. 5. Temperature dependence of the resistivities of (a) Mn_3SnC and (b) $Mn_{3.1}Sn_{0.9}C$ compounds at zero field (the solid symbols) and at a magnetic field of 5 T (the open symbols).

occurs and thus no large MR effect exists for the $Mn_{3+x}Sn_{1-x}C$ compounds. It is thought that when an external magnetic field is applied, a field-induced metamagnetic phase transition could occur below/near the transition temperature for a magnetic transition from a FM (or FI) state to a pure AFM state. Therefore, the appearance of a single and stable AFM phase at low temperatures and correspondingly the occurrence of a magnetic phase transition of AFM-FM (or FI) type are important for observation of a large MR effect in intermetallic compounds. For this purpose, the effect of Zn substitution for Sn on magnetic, transport, and magnetotransport properties of the Mn_3SnC compound will be studied in the remainder of this paper.

B. $Mn_3Zn_ySn_{1-y}C$ ($0 \leq y \leq 0.9$)

XRD measurements indicate that with Zn substitution for Sn in the Mn_3SnC compound, there is no change in the crystal structure. However, since the boiling point of Zn (1180 K) is relatively much lower than that of Sn (2876 K) and Mn (2335 K), there exist some deviation in the compositions because of the volatilization of Zn, as certified by the results of Energy Dispersive Spectrum (EDS). Figure 6 shows the temperature dependence of susceptibility of several $Mn_3Zn_ySn_{1-y}C$ compounds, while Fig. 7 represents the variation of Mn—Mn distance with y concentration. For the compounds with $y < 0.4$, the susceptibility curves are similar to that of Mn_3SnC which undergoes a magnetic phase transition from the PM to the FI state. With increasing the Zn concentration, the Curie temperature T_C decreases from 260 K for Mn_3SnC to 188 K for $Mn_3Zn_{0.4}Sn_{0.6}C$. However, it is evident that the Zn substitution for Sn causes the presence of a pure AFM phase at about 170 K, 142 K for $Mn_3Zn_{0.4}Sn_{0.6}C$ and $Mn_3Zn_{0.5}Sn_{0.5}C$ compounds, respectively. Meanwhile, the magnetic state just below the Curie

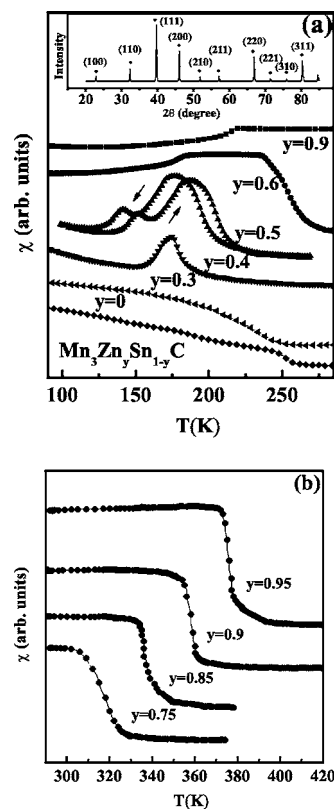


FIG. 6. Temperature dependence of the susceptibility of $Mn_3Zn_ySn_{1-y}C$ compounds. The inset in Fig. 6(a) shows the XRD result of $Mn_3Zn_{0.5}Sn_{0.5}C$ compound. The values for the transition temperatures and the Curie temperatures of these compounds are represented in Table I.

temperature becomes the FM one.¹⁶ A single peak at about 170 K in the susceptibility curve of $Mn_3Zn_{0.4}Sn_{0.6}C$ corresponds to the FM-AFM transition temperature T_{FM-AFM} . Two peaks appear at about 142 and 168 K in the susceptibility curve of $Mn_3Zn_{0.5}Sn_{0.5}C$. The higher one corresponds to the FM-FI transition (T_{FM-FI}), while the lower one corresponds to the FI-AFM transition (T_{FI-AFM}). The inset of Fig. 6(a) shows the XRD pattern of $Mn_3Zn_{0.5}Sn_{0.5}C$ compound, indicating that the sample displays peaks characteristic for the cubic perovskite-type structure without impurity phase. The transition from the FM state at high temperatures to the AFM state at low temperatures is a gradual one, passing through a FI state, and the Curie temperature T_C is 200 K. An obvious

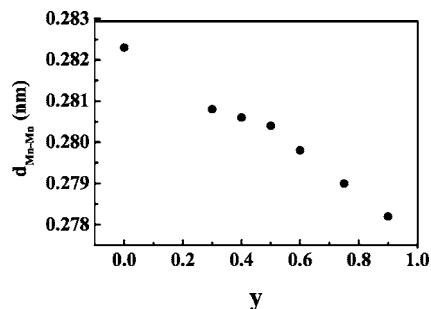


FIG. 7. Composition dependence of Mn—Mn distance of $Mn_3Zn_ySn_{1-y}C$ compounds.

TABLE I. The transition temperature and Curie temperature of $\text{Mn}_3\text{Zn}_y\text{Sn}_{1-y}\text{C}$ compounds. FM, AFM, and FI represent ferromagnetic, antiferromagnetic, and ferrimagnetic, respectively.

Nominal composition	Transition temperature (K)	Curie temperature (K)
Mn_3SnC	–	260
$\text{Mn}_3\text{Zn}_{0.3}\text{Sn}_{0.7}\text{C}$	–	248
$\text{Mn}_3\text{Zn}_{0.4}\text{Sn}_{0.6}\text{C}$	170 (FM-AFM)	188
$\text{Mn}_3\text{Zn}_{0.5}\text{Sn}_{0.5}\text{C}$	168 (FM-FI)	200
	142 (FI-AFM)	
$\text{Mn}_3\text{Zn}_{0.6}\text{Sn}_{0.4}\text{C}$	184 (FM-FI)	265
$\text{Mn}_3\text{Zn}_{0.75}\text{Sn}_{0.25}\text{C}$	205 (FM-FI)	325
$\text{Mn}_3\text{Zn}_{0.9}\text{Sn}_{0.1}\text{C}$	220 (FM-FI)	360

thermal hysteresis of susceptibility (only the thermal hysteresis curve for $y=0.5$ is shown in Fig. 6) can be observed in the cooling and warming cycle, indicating there undergoes a first-order transition. For the compounds with $y>0.5$, the susceptibility curves look like that of Mn_3ZnC , which only experiences a FM-FI transition below its Curie temperature. As $y>0.5$, the Curie temperature T_C increases with the Zn concentration [see Fig. 6(b)].

The transition temperatures and Curie temperatures of all the $\text{Mn}_3\text{Zn}_y\text{Sn}_{1-y}\text{C}$ compounds are listed in Table I. The transition temperature ($T_{\text{AF-FM}}$ or $T_{\text{AF-FI}}$) is determined by the peak value of the susceptibility curve. The behavior observed in $\text{Mn}_3\text{Zn}_y\text{Sn}_{1-y}\text{C}$ is consistent with the magnetic phase diagram deduced by Lorthioir *et al.*^{16,20} From the Zn concentration dependence of Mn moment at 0 K for $\text{Mn}_3\text{Zn}_y\text{Sn}_{1-y}\text{C}$,¹⁶ it can be seen that the magnetization reaches the minimum at $y=0.5$. This indicates the presence of an AFM structure, in good agreement with the results above. Substitution of Sn by Zn can cause the change of the crystal lattice parameters and correspondingly the atomic distance $d_{\text{Mn-Mn}}$. Guillaud²¹ suggested that in a number of manganese compounds, i.e., Mn_2Sb , Mn_2As , MnBi , etc., the lower limit of the distance between manganese atoms which would give a positive (ferromagnetic) exchange interaction is about 2.81 Å and that for Mn_4N , the distance of 2.72 Å would give rise to negative (ferrimagnetic or antiferromagnetic) interaction. However, these values are only empirical estimations from the experimental data at room temperature, not accurate criterions. For the present $\text{Mn}_3\text{Zn}_y\text{Sn}_{1-y}\text{C}$ system, according to Fig. 6, all of the compounds have a negative interaction at low temperatures, which are in either ferrimagnetic or antiferromagnetic state. At room temperature, the ferromagnetic behavior occurs for $y>0.6$ (with the Mn—Mn distance of 0.280–0.278 Å, see Fig. 7), while the paramagnetic behavior exists for $y<0.6$. It seems that the empirical estimation of the critical distance (2.72 Å) for Mn_4N is more suitable for the present system than that obtained for Mn_2Sb , Mn_2As , and MnBi .²¹ Nevertheless, it is clear now that the sign and magnitude of the Mn—Mn interaction may sensitively depend on the Mn—Mn distance. For instance, for $y=0.5$, the compound experiences magnetic phase

transitions of paramagnetic-ferromagnetic-ferrimagnetic-antiferromagnetic, when the temperature is lowered from room temperature to 4.2 K. Moreover, according to Gerasimov *et al.*²² there exists a critical distance d_c between Mn atoms. When $d_{\text{Mn-Mn}} \sim d_c$, the electron band structure of the compounds changes considerably. In particular, the Mn—Mn exchange interaction is supposed to depend on the DOS of electrons at the Fermi level.²³ In the vicinity of the critical Mn—Mn distance, the DOS is considered to vary strongly, which results in a change in the type of the Mn—Mn magnetic ordering. Therefore, it is understandable that the Zn substitution for Sn leads to the formation of the AFM ordering at low temperatures.

The temperature dependences of the resistivities of $\text{Mn}_3\text{Zn}_{0.5}\text{Sn}_{0.5}\text{C}$ compound at zero field and at a magnetic field of 5 and 12 T are shown in Fig. 8(a). At zero field, the resistivities first decrease, then rise at about 168 K, reaching a maximum, and finally decrease with decreasing temperature. The temperature, where the resistivity is minimum, corresponds to the FM-FI phase transition temperature $T_{\text{FM-FI}}$ (=168 K) observed in the susceptibility curve as shown in Fig. 6. When magnetic fields are applied, two minima appear in the temperature dependence of the resistivity. In the temperature region (about 100–150 K) for the metamagnetic transition, the system does not acquire a collinear FM state even under the applied field of 12 T [as can be seen from field dependence of the magnetization shown in Fig. 9(b)]. But at 175 K, the magnetization is almost saturated. So the resistivity behaviors are different, corresponding to different magnetic structures at different temperatures/applied fields. The minimum at higher temperature originates from the transition from saturated state to unsaturated state, at a certain magnetic field, while the one at lower temperature corresponds to the transition from unsaturated state to AFM state. Both the two minima shift to lower temperatures with the magnetic field increasing from 5 to 12 T, which indicate that the higher applied field tends to collapse the AFM state and stabilize the collinear FM state at comparatively lower temperatures. Figure 8(c) shows the temperature dependence of the MR ratio $\Delta\rho/\rho=[(\rho_H-\rho_0)/\rho_0]$ of $\text{Mn}_3\text{Zn}_{0.5}\text{Sn}_{0.5}\text{C}$ compound at a field of 5 and 12 T. At an applied field of 5 T, the MR ratio $\Delta\rho/\rho$ is small at low temperatures, because of the existence of the stable AFM state. When the temperature increases up to a certain temperature, the AFM structure becomes unstable at the external field. Namely, a metamagnetic transition occurs at a certain magnetic field, resulting in a rapid increase of $-\Delta\rho/\rho$ value. Peak temperatures of 134 and 95 K for applied field of 5 and 12 T are observed with the value of $-\Delta\rho/\rho$ of 15% and 34%, respectively. Above the peak temperature, $-\Delta\rho/\rho$ drops rapidly with increasing temperature because the stable FM state forms, and at higher temperatures the metamagnetic transition trends not to occur when the magnetic field is applied. Similar results can be obtained for the compound $\text{Mn}_3\text{Zn}_{0.4}\text{Sn}_{0.6}\text{C}$ [see Figs. 8(b) and 8(d)], in which the MR ratio of 6% and 16% are observed at applied field of 5 and 12 T.

To better understand the magnetotransport behavior, the magnetic field dependence of the MR ratio $\Delta\rho/\rho$ and the magnetization of $\text{Mn}_3\text{Zn}_{0.5}\text{Sn}_{0.5}\text{C}$ at different temperatures

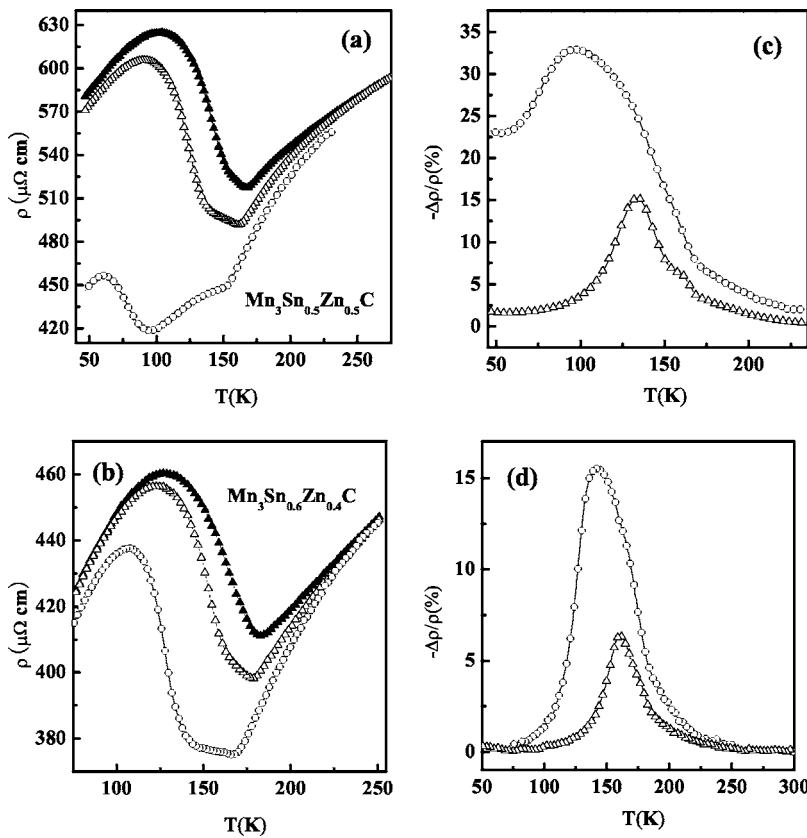


FIG. 8. Temperature dependence of the resistivities of (a) $\text{Mn}_3\text{Zn}_{0.5}\text{Sn}_{0.5}\text{C}$ and (b) $\text{Mn}_3\text{Zn}_{0.4}\text{Sn}_{0.6}\text{C}$ compound at zero field (the solid symbols) and at a magnetic field of 5 T (the open triangle symbols) and 12 T (the open circle symbols). (c) and (d) represent the temperature dependence of the MR ratio $\Delta\rho/\rho=[(\rho_H-\rho_0)/\rho_0]$ of the $\text{Mn}_3\text{Zn}_{0.5}\text{Sn}_{0.5}\text{C}$ and $\text{Mn}_3\text{Zn}_{0.4}\text{Sn}_{0.6}\text{C}$ compounds at a field of 5 T (the open triangle symbols) and 12 T (the open circle symbols), respectively.

are represented in Figs. 9(a) and 9(b). At 4.2 K, $\Delta\rho/\rho$ is small (less than 7% at the maximum applied field of 12 T). Between 50 and 145 K, it develops drastically around the critical field (B_m), indicating that the compound undergoes a metamagnetic transition from an AFM state to a FM state. A similar transition related to MR has been observed in $\text{Ce}(\text{Fe}, \text{Al})_2$, $\text{Ce}(\text{Fe}, \text{Ru})_2$, UCu_2Ge_2 , Mn_3GaC , $(\text{Mn}, \text{Cr})_2\text{Sb}$, and $\text{Mn}_2(\text{Sb}, \text{Sn})$ compounds.^{24–29} The critical field (B_m), at which a negative MR develops, decreases with increasing the temperature up to 145 K. Above the metamagnetic transition, the MR does not saturate up to the maximum applied field of 12 T. This indicates that the system does not acquire a collinear FM state but rather goes into a canted FM state in the range of fields studied. The inset of Fig. 9(a) shows an obvious magnetic hysteresis at 4.2 K. The field dependence of the magnetization at a few temperatures is shown in Fig. 9(b). There is not a rapid increase in the magnetization at a critical field as observed in $\text{Ce}(\text{Fe}, \text{Co})_2$ and Mn_3GaC compounds. Usually, a sharp increase of magnetization is observed for a first-order magnetization process. No sharp increase of magnetization might be ascribed to the random distribution of the grains of our polycrystalline samples.³⁰ However, the inflection points, which coincide with the metamagnetic transition, can be observed. The magnetization is not saturated up to 12 T in this temperature range. The metamagnetic field (B_m) decreases with increasing temperature and a hysteresis is observed at 4.2 K as expected for a first-order transition. A recent study illustrated that in most cases (i.e., at temperatures low enough), the field-induced magnetic phase transition is of the first order.³¹ The field-induced magnetic phase transition can be of the second order

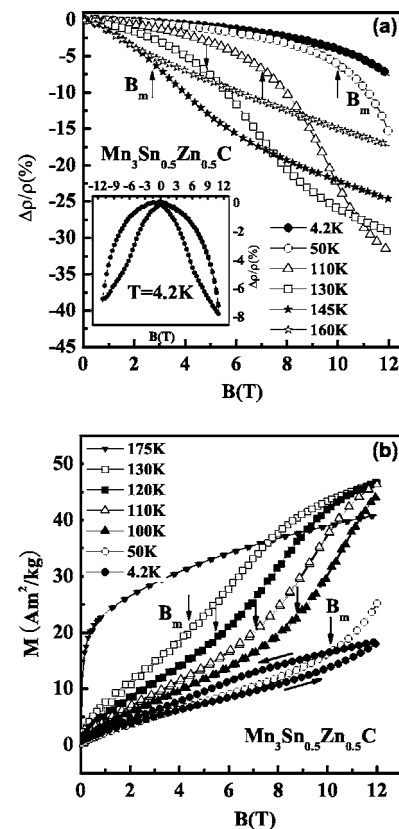


FIG. 9. Field dependence of (a) the magnetoresistance and (b) the magnetization of $\text{Mn}_3\text{Zn}_{0.5}\text{Sn}_{0.5}\text{C}$ compound at different temperatures.

only at a critical temperature as previously denoted by T_{SOMP} (normally at a relatively high temperature).³¹ Therefore, we are convinced that the metamagnetic phase transition in the present system is of the first order (at least at most of temperatures).

The sharp rise of the resistivities below the AFM ordering temperature $T_{\text{FM-AFM}}$ in $\text{Mn}_3\text{Zn}_{0.4}\text{Sn}_{0.6}\text{C}$ (or $T_{\text{FI-AFM}}$ in $\text{Mn}_3\text{Zn}_{0.5}\text{Sn}_{0.5}\text{C}$) is tentatively ascribed to the super-zone gap, as a consequence of an additional periodicity in the AFM state.³²⁻³⁴ This is a common behavior for the magnetic part of the resistivity in metallic magnets with periodic non-collinear spin structures.³⁴ The rise in resistivity is the result of the change in the effective number of conduction electrons, due to the change of the DOS near the Fermi level caused by the new periodicity (the spin order periodicity) which appears on top of the crystalline periodicity at low temperatures. The super-zone gap can be suppressed when a sufficiently high magnetic field is applied. In this experiment, an applied field of 12 T stabilizes the FM state and suppresses the formation of a super-zone gap to lower temperatures. Namely, the applied field shifts the AFM ordering temperature to lower temperatures and eventually results in the negative MR.⁹ Recently, the mechanism of the large magnetoresistance and the first-order nature of the metamagnetic transition in an intermetallic compound $\text{Mn}_2\text{Sb}_{0.95}\text{Sn}_{0.05}$ were investigated in details.³⁵ It was confirmed experimentally that the large magnetoresistance effect in intermetallic

compounds is originated from the reconstruction of the Fermi surface, due to the collapse of the super-zone gap after the metamagnetic transition.³⁵

IV. SUMMARY

The magnetic, transport and magnetotransport properties of the $\text{Mn}_{3+x}\text{Sn}_{1-x}\text{C}$ ($0 \leq x \leq 0.4$) and $\text{Mn}_3\text{Zn}_y\text{Sn}_{1-y}\text{C}$ ($0 \leq y \leq 0.9$) compounds have been studied systematically. The $\text{Mn}_{3+x}\text{Sn}_{1-x}\text{C}$ ($x \leq 0.1$) compounds show an abrupt increase in the temperature dependence of the resistivity near the Curie temperature, which originates from the sharp decrease of the effective number of conduction electrons, resulting from the shift of the Fermi surface. Partial substitution of Sn by Zn can cause the transition from the FM (or FI) state to the AFM one at about 170 K, 142 K for $\text{Mn}_3\text{Zn}_{0.4}\text{Sn}_{0.6}\text{C}$ and $\text{Mn}_3\text{Zn}_{0.5}\text{Sn}_{0.5}\text{C}$ compounds, respectively, which strongly affects the transport property. Moreover, a significant magnetoresistance as large as 34% is observed in accordance with the metamagnetic transition. The results are discussed on the basis of the reconstruction of the Fermi surface, due to the suppression of the formation of super-zone gap after the metamagnetic transition.

This work has been supported by the National Natural Science Foundation of China under Grant No. 50332020.

-
- ¹M. N. Baibich, J. M. Broto, A. Fert, F. Nguyen van Dau, F. Petroff, P. Etienne, G. Creuzet, A. Frederich, and J. Chazeles, *Phys. Rev. Lett.* **61**, 2472 (1988).
- ²S. S. P. Parkin, Z. G. Li, and D. J. Smith, *Appl. Phys. Lett.* **58**, 2710 (1991).
- ³S. S. P. Parkin, R. Bhadra, and K. P. Roche, *Phys. Rev. Lett.* **66**, 2152 (1991).
- ⁴F. Petroff, A. Barthelemy, D. H. Mosca, D. K. Lottis, A. Fert, P. A. Schroeder, W. P. Pratt, R. Loloee, and S. Lequien, *Phys. Rev. B* **44**, 5355 (1991).
- ⁵J. Q. Xiao, J. S. Jiang, and C. L. Chien, *Phys. Rev. Lett.* **68**, 3749 (1992).
- ⁶A. E. Berkowitz, J. R. Mitchell, M. J. Carey, A. P. Young, S. Zhang, F. E. Spada, F. T. Parker, A. Hutten, and G. Thomas, *Phys. Rev. Lett.* **68**, 3745 (1992).
- ⁷V. Sechovsky, L. Havela, K. Prokes, H. Nakotte, F. R. de Boer, and E. Brück, *J. Appl. Phys.* **76**, 6913 (1994).
- ⁸K. Kamishima, T. Goto, H. Nakagawa, N. Miura, M. Ohashi, N. Mori, T. Sasaki, and T. Kanomata, *Phys. Rev. B* **63**, 024426 (2001).
- ⁹W. S. Kim, E. O. Chi, J. C. Kim, H. S. Choi, and N. H. Hur, *Solid State Commun.* **119**, 507 (2001).
- ¹⁰T. He, Q. Huang, A. P. Ramirez, Y. Wang, K. A. Reran, N. Rogado, M. A. Hayward, M. K. Haas, J. S. Slusky, K. Inumara, H. W. Zandbergen, N. P. Ong, and R. J. Cava, *Nature (London)* **411**, 54 (2001).
- ¹¹D. Fruchart, E. F. Bertaut, F. Sayetat, M. Nasr Eddine, R. Fruchart, and J. P. Senateur, *Solid State Commun.* **8**, 91 (1970).
- ¹²J. H. Shim, S. K. Kwon, and B. I. Min, *Phys. Rev. B* **66**, 020406(R) (2002).
- ¹³D. Fruchart and E. F. Bertaut, *J. Phys. Soc. Jpn.* **44**, 781 (1978).
- ¹⁴T. Kaneko, T. Kanomata, and K. Shirakawa, *J. Phys. Soc. Jpn.* **56**, 4047 (1987).
- ¹⁵D. Fruchart, E. F. Bertaut, B. Le Clerc, Le Dang Khoi, P. Veillet, G. Lorthioir, E. Fruchart, and R. Fruchart, *J. Solid State Chem.* **8**, 182-188 (1973).
- ¹⁶G. Lorthioir, E. Fruchart, M. Nardin, P. L'Heritier, and R. Fruchart, *Mater. Res. Bull.* **8**, 1027 (1973).
- ¹⁷E. Fruchart, G. Lorthioir, and R. Fruchart, *C. R. Acad. Sci. (Paris)* **275**, c-1415 (1972).
- ¹⁸K. Motizuki and H. Nagai, *J. Phys. C* **21**, 5251 (1988).
- ¹⁹R. G. Butters and H. P. Myers, *Philos. Mag.* **46**, 132 (1955).
- ²⁰Compared with the magnetic phase diagram in Ref. 16, there exist some deviation in transition temperatures, which might result from the slight deviation in the compositions of the as-prepared samples by the different preparation methods. Note that y in this work corresponds to $1-x$ in Ref. 16. Nevertheless, it is clear that the complicated magnetic structure in Mn_3SnC does not exist in the $\text{Mn}_3\text{Zn}_y\text{Sn}_{1-y}\text{C}$ compounds with $y \geq 0.4$.
- ²¹C. Guillaud, *Rev. Mod. Phys.* **25**, 119 (1953).
- ²²E. G. Gerasimov, V. S. Gaviko, V. N. Neverov, and A. V. Korolyov, *J. Alloys Compd.* **343**, 14 (2002).
- ²³H. Fujii, M. Isoda, T. Okamoto, T. Shigeoka, and N. Iwata, *J. Magn. Magn. Mater.* **54-57**, 1345 (1986).
- ²⁴S. Radha, S. B. Roy, A. K. Nigam, and G. Chandra, *Phys. Rev. B* **50**, 6866 (1994).

- ²⁵H. P. Kunkel, X. Z. Zhou, P. A. Stampe, J. A. Cowen, and G. Williams, *Phys. Rev. B* **53**, 15099 (1996).
- ²⁶A. K. Nigam, S. B. Roy, and G. Chandra, *Phys. Rev. B* **49**, 1127 (1994).
- ²⁷S. Y. Zhang, P. Zhao, Z. H. Cheng, R. W. Li, J. R. Sun, H. W. Zhang, and B. G. Shen, *Phys. Rev. B* **64**, 212404 (2000).
- ²⁸Y. Nagata, T. Hagi, S. Yashiro, H. Samata, and S. Abe, *J. Alloys Compd.* **292**, 11 (1999).
- ²⁹Y. Q. Zhang and Z. D. Zhang, *Phys. Rev. B* **67**, 132405 (2003).
- ³⁰Z. D. Zhang, Y. K. Huang, X. K. Sun, Y. C. Chuang, F. R. de Boer, and R. J. Radwański, *J. Less-Common Met.* **152**, 67 (1989).
- ³¹T. Zhao, Z. D. Zhang, W. Liu, X. K. Sun, and R. Grössinger, *Phys. Rev. B* **67**, 014419 (2003).
- ³²M. H. Jung, D. T. Adroja, N. Kikugawa, T. Takabatake, I. Oguro, S. Kawasaki, and K. Kindo, *Phys. Rev. B* **62**, 13 860 (2000).
- ³³H. Fukuda, H. Fujii, H. Kamura, Y. Hasegawa, T. Ekino, N. Kikugawa, T. Suzuki, and T. Fujita, *Phys. Rev. B* **63**, 054405 (2001).
- ³⁴J. Y. Chan, S. M. Kauzlarich, P. Klavins, R. N. Shelton, and D. J. Webb, *Phys. Rev. B* **57**, R8103 (1998).
- ³⁵Y. Q. Zhang, Z. D. Zhang, and J. Aarts, *Phys. Rev. B* **70**, 132407 (2004).